High-Isolation Leaky-Wave Array Antenna Based on CRLH-Metamaterial Implemented on SIW with ±30° Frequency Beam-Scanning Capability at Millimetre-Waves

Mohammad Alibakhshikenari [1,*], Bal Singh Virdee [2], Chan H. See [3,4], Raed A. Abd-Alhameed [5], Francisco Falcone [6] and Ernesto Limiti [1]

[1] Electronic Engineering Department, University of Rome "Tor Vergata", Via del Politecnico 1, 00133 Rome, Italy; limiti@ing.uniroma2.it
[2] Center for Communications Technology, School of Computing & Digital Media, London Metropolitan University, London N7 8DB, UK; b.virdee@londonmet.ac.uk
[3] School of Engineering & the Built Environment, Edinburgh Napier University, 10 Colinton Rd., Edinburgh EH10 5DT, UK; C.See@napier.ac.uk
[4] School of Engineering, University of Bolton, Deane Road, Bolton BL3 5AB, UK
[5] Faculty of Engineering & Informatics, University of Bradford, Bradford, West Yorkshire BD7 1DP, UK; R.A.A.Abd@Bradford.ac.uk
[6] Electrical and Electronic Engineering Department, Public University of Navarre, 31006 Pamplona, Spain; francisco.falcone@unavarra.es
* Correspondence: alibakhshikenari@ing.uniroma2.it

Abstract: The paper presents a feasibility study on the design of a new metamaterial leaky-wave antenna (MTM-LWA) used in the construction of a 1 × 2 array which is implemented using substrate-integrated waveguide (SIW) technology for millimetre-wave beamforming applications. The proposed 1 × 2 array antenna consists of two LWAs with metamaterial unit-cells etched on the top surface of the SIW. The metamaterial unit-cell, which is an E-shaped transverse slot, causes leakage loss and interrupts current flow over SIW to enhance the array's performance. The dimensions of the LWA are 40 × 10 × 0.75 mm³. Mutual-coupling between the array elements is suppressed by incorporating a metamaterial shield (MTM-shield) between the two antennas in the array. The LWA operates over a frequency range of 55–65 GHz, which is corresponding to 16.66% fractional bandwidth. The array is shown to exhibit beam-scanning of ±30° over its operating frequency range. Radiation gain in the backward (−30°), broadside (0°), and forward (+30°) directions are 8.5 dBi, 10.1 dBi, and 9.5 dBi, respectively. The decoupling slab is shown to have minimal effect on the array's performance in terms of impedance bandwidth and radiation specifications. The MTM-shield is shown to suppress the mutual coupling by ~25 dB and to improve the radiation gain and efficiency by ~1 dBi and ~13% on average, respectively.

Keywords: Metamaterials (MTM), leaky-wave antenna (LWA), antenna arrays; substrate integrated waveguide (SIW), transverse slots; beam-scanning; mutual coupling isolation; millimetre-wave; composite right/left-handed transmission line (CRLH-TL).

1. Introduction

Leaky-wave antennas (LWAs) are travelling wave antennas with electrically large radiating aperture [1,2]. Such antennas can provide high gain directive beam without using a complex feeding network [3,4]. The advantage of LWA over a conventional array antenna is a simple feed structure with low loss [5–7]. Conventional planar LWAs radiate higher order modes in the forward direction

[8]. However, the periodic structure-based LWA can radiate in both forward and backward directions. It has been shown that metamaterial-based LWA designs can achieve a continuous main beam scanning from the backward to the forward direction as a function of frequency [9]. Various LWA designs based on metamaterial structures have been considered in the past. Such designs include (1) an LWA with a composite right/left-hand (CRLH)-folded substrate-integrated waveguide (SIW) structure that is shown to provide beam scanning from of -58° to 65° with a gain of 1 dBi [10]; (2) an interdigital-shaped slotted-SIW-based LWA that is reported to achieve a scanning angle of −60° to 70° with gain of around 8 dBi [11]; (3) a CRLH LWA based on a rectangular waveguide structure that has been demonstrated for a continuous main beam scanning range from −70° to 70° with gain of 8.64 dBi [12]; and (4) a planar slotted SIW LWA that provides a scanning range of −66° to 78° with consistent gain [13].

In this paper, a new type of LWA in array configuration is proposed based on SIW with metamaterial inclusions for millimetre-wave applications. Mutual coupling between the closely-spaced antennas in the array can undermine the array's performance. To circumvent this, a metamaterial shield is embedded between the two LWAs. With this approach, mutual coupling is shown to reduce by an average of ~25 dB over the array's operating frequency range. Engraved on the upper layer of the SIW LWA are several metamaterial unit-cells comprising of transverse E-shaped slots. Dimensions of the LWAs were modified for optimum array performance.

## 2. Design Process of The Proposed Mtm-Lwa Array Based On Siw

The proposed 1 × 2 array antenna based on MTM-LWA implemented on SIW technology is designed on a RO3003 dielectric substrate with ε_r = 3.0, tanδ = 0.0010 and thickness of 0.75 mm. Figure 1 displays the layout of the proposed array structure that is constructed with two MTM-LWA on SIW. Engraved on the top of each SIW antenna are several metamaterial unit-cells consisting of transverse E-shaped slots. Leakage loss at the slots interrupts the current flow over SIW, which is shown to enhance the array's impedance bandwidth and beamwidth that scans as a function of frequency. In the structure, the transverse slots behave as series left-handed capacitance and the grounded via holes acts as shunt left-handed inductors.
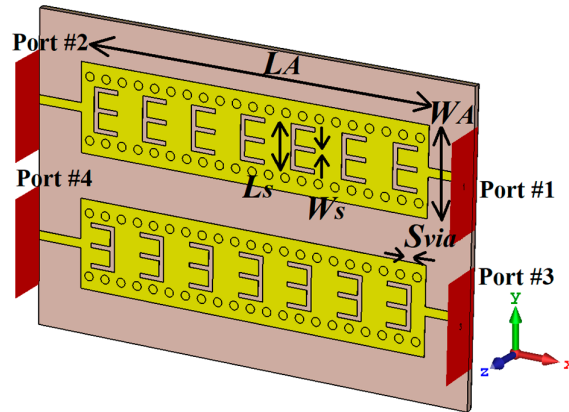

(**a**)
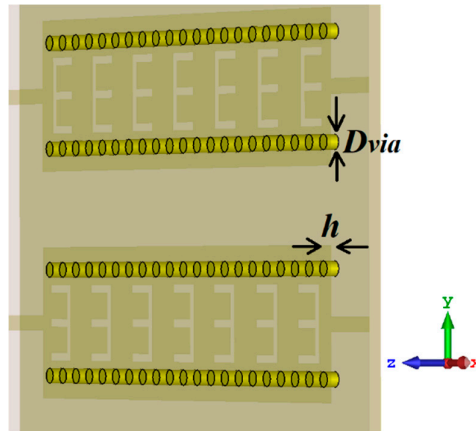
(**b**)
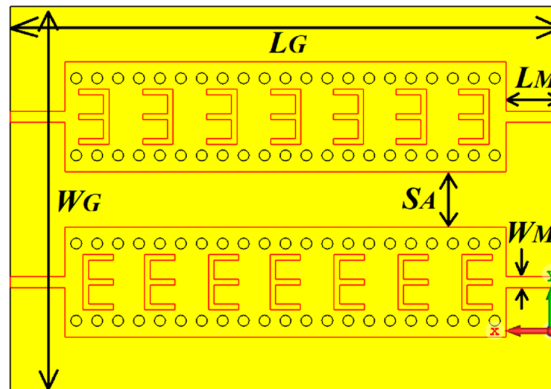
(**c**)

Figure 1. Proposed 1 × 2 array antenna based on MTM-LWA using SIW technology. (**a**) Top view; (**b**) view to show the Substrate integrated waveguide slots; (**c**) back side to show the ground plane.

The structural parameters of the MTM-LWA array are summarized in Table 1. Each antenna has dimensions of 40 × 10 × 0.75 mm³. The overall ground plane dimensions are 50 × 35 × 0.75 mm³. The S-parameter responses of the proposed array antenna are exhibited in Figure 2, which shows it operates throughout the frequency range of 55–65 GHz, which corresponds to 16.66% fractional bandwidth.

Table 1. Structural parameters of the array.

| Structural Parameters	Dimensions (units in mm)
L_A	40
W_A	10
L_G	50
W_G	35
L_S	5
W_S	0.5
$Dvia$	0.5
$Svia$	0.5
S_A	5
L_M	5
W_M	1
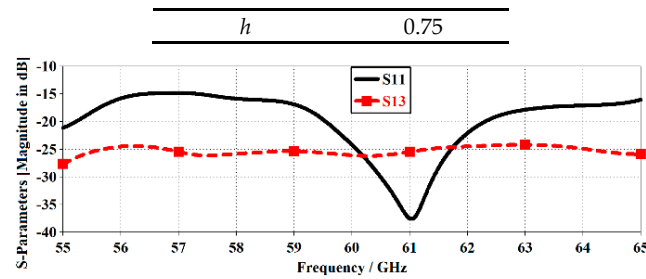
Figure 2. S-parameter responses of the proposed array antennas. Since the structure is symmetrical, we have not plotted all curves.

Radiation gain patterns of the proposed array antenna at three spot frequencies within its operating frequency range are plotted in Figure 3. It is evident that the array antenna is capable of beam-scanning from −30° to +30° with backward radiation at −30°, broadside radiation at $0°$, and forward radiation at +30°. In backward, broadside, and forward directions, the gain is 8.5, 10.1, and 9.5 dBi, respectively.

(a)

(b)

(c)
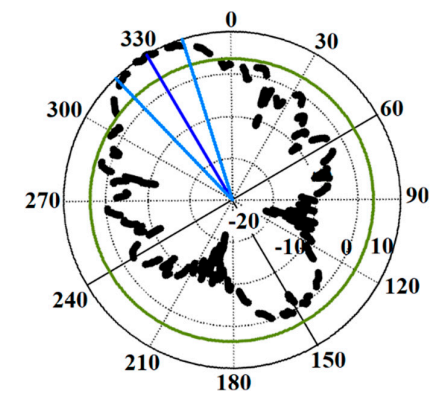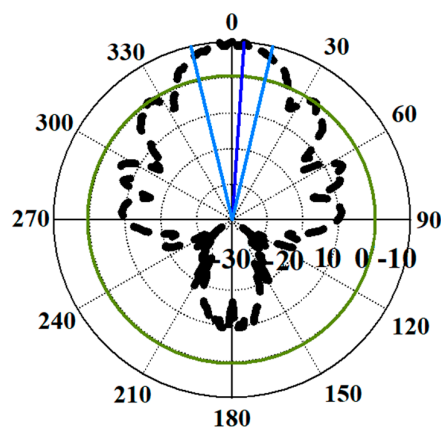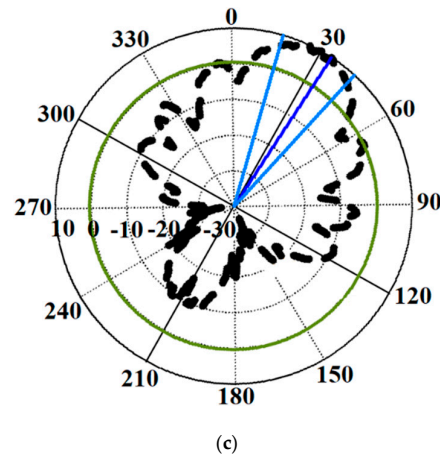
Figure 3. Radiation characteristics of the proposed 1 × 2 MTM-LWA array at 55 GHz, 60 GHz, and 65 GHz. (**a**) Backward-radiation at 55 GHz; (**b**) broadside-radiation at 60 GHz; (**c**) forward-radiation at 65 GHz.

## 3. Suppress the Mutual Coupling Between the Closely Spaced Mtm-Lwa Arrays

Mutual coupling between closely-spaced radiation elements can severely undermine the array's radiation performances. Here the isolation between the two MTM-LWAs is increased by introducing a metamaterial shield which is based on the SIW structure, as indicated in Figure 4. It comprises of transverse slots that are tapered. The slots have a width of 0.5 mm and essentially play the role of the series left-handed capacitances (C_L), where the metallic via-holes with diameter of 0.25 mm act as shunt left-handed inductances (L_L). The MTM-shield suppresses surface waves created by the LWAs to increase isolation between the two antennas in the array. The overall dimensions of the shield are 40 × 4 mm².

Figure 5 shows the S-parameter response before and after applying the MTM-shield. After applying MTM-shield, the minimum, average and maximum suppression observed are 8 dB, ~25 dB, and 42.5 dB, respectively. This shows the effectiveness of the proposed isolation technique. The shield has no influence on the reflection coefficient response which is $S_{11} \le -10$ dB.

Radiation patterns of the proposed antenna arrays with no and with MTM-shield through its operational bandwidth at spot frequencies of 55 GHz, 60 GHz & 65 GHz are plotted in Figure 6. It is clear from this figure that with the shield the cross-polarized radiation over its operating range is substantially reduced. The average gain of the co-polarized radiation is only marginally affected. All details are tabulated in Table 2.

In addition, the radiation gain and efficiency curves over frequency bandwidth for both antennas without and with the proposed shield are shown in Figure 7. Obviously, after realizing the metamaterial shield based on SIW, the radiation gain and efficiency performances improved by ~1dBi and ~13% on average, respectively.

Surface current density distributions without and with the MTM-shield are exhibited in Figure 8. This figure shows that the MTM-shield is an effective EM band-gap structure to remarkably block surface currents from EM interacting with adjacent radiation elements in the antenna array. Destructive influences of surface currents in the antenna are dramatically suppressed from effecting the far-field of the array antennas.
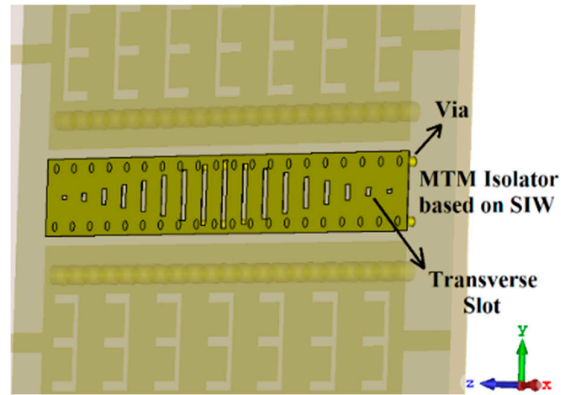
(**a**)
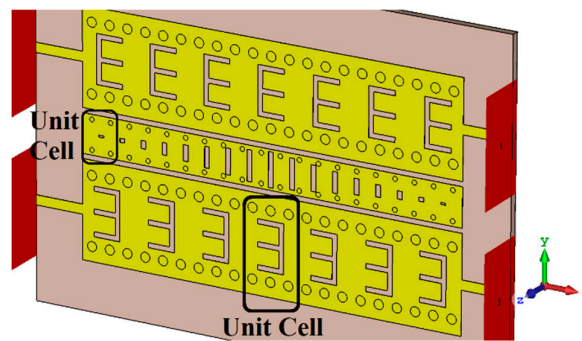
(**b**)
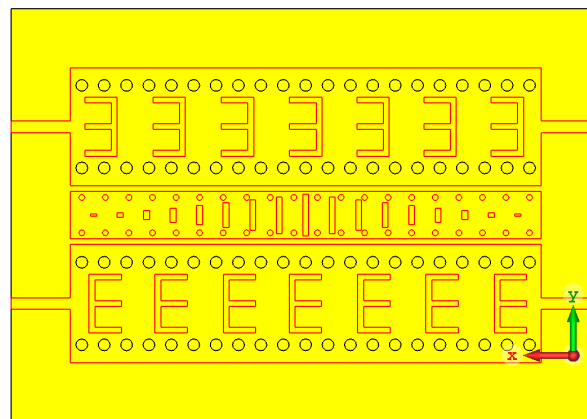
(**c**)

Figure 4. Proposed SIW-based leaky-wave antenna array with MTM-shield. (**a**) Proposed MTM-SIW shield located between the array antennas; (**b**) top-view of the leaky-wave array antennas; (**c**) back-side to show ground plane.
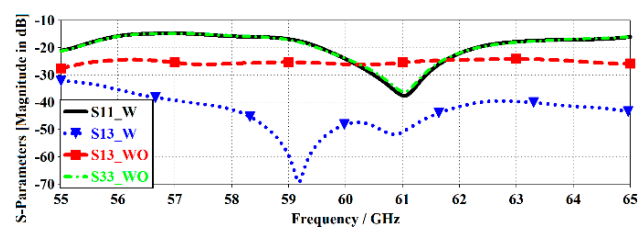
Figure 5. Reflection and transition coefficients of the proposed antenna array before and after applying the MTM-shield. Since the structure is symmetrical, we have not plotted all curves.
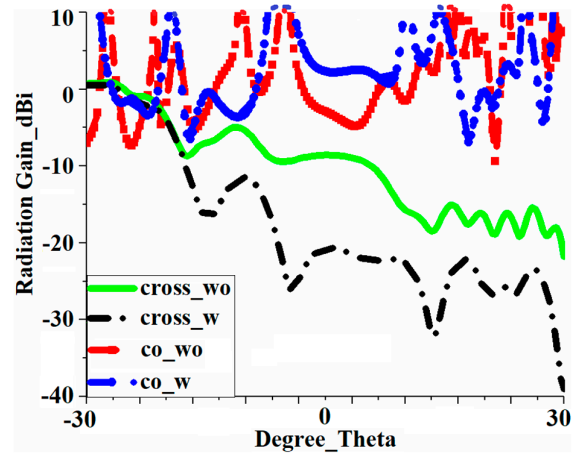
@ 55 GHz
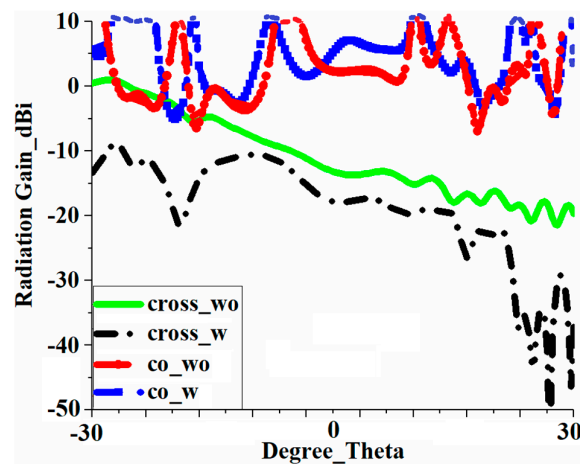
@ 60 GHz
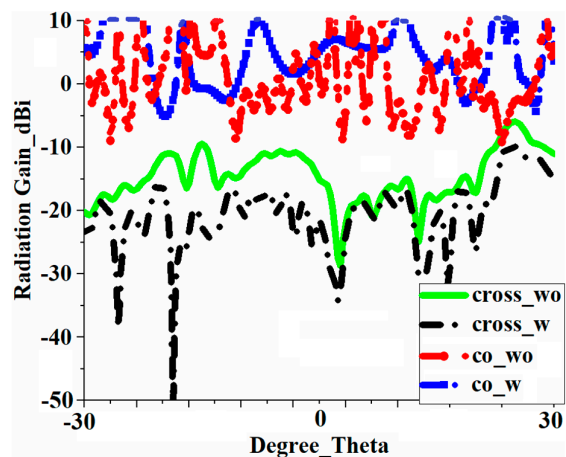
@ 65 GHz

Figure 6. Co- and cross-polarized radiation gain patterns of the proposed structure without (WO) and with (W) metamaterial-shield.

(a)

(b)
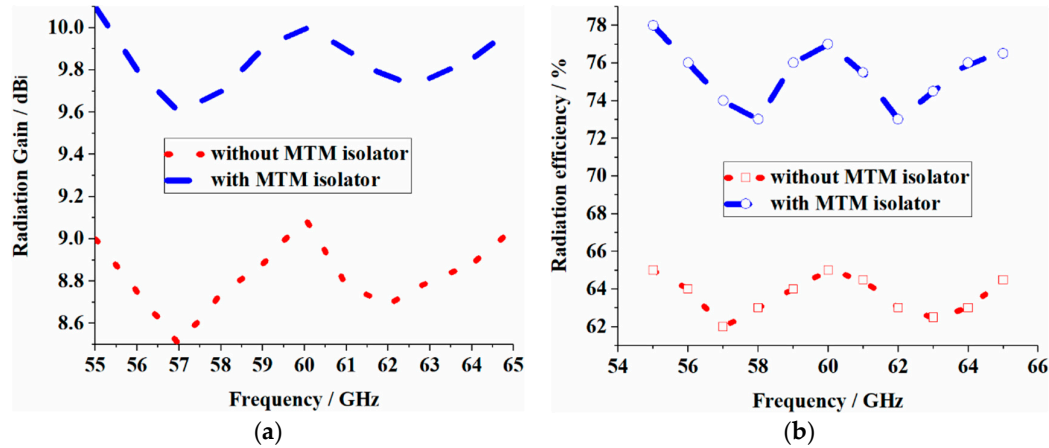
Figure 7. Radiation gain and efficiency curves over frequency band for both cases with no and with MTM shield. (**a**) Radiation-gain; (**b**) Radiation-efficiency.

Table 2. Radiation properties.

Radiation Gain		
	Without MTM	**With MTM**
Minimum	8.69 dBi	9.6 dBi
Maximum	9.11 dBi	10.16 dBi
Average	8.90 dBi	9.86 dBi
Improvement in Average	~1 dBi	
Radiation Efficiency		
	Without MTM	With MTM
Minimum	62.53%	73.44%
Maximum	65.21%	78.12%
Average	63.5%	76.38
Improvement in Average	~13%	

(a)

(b)
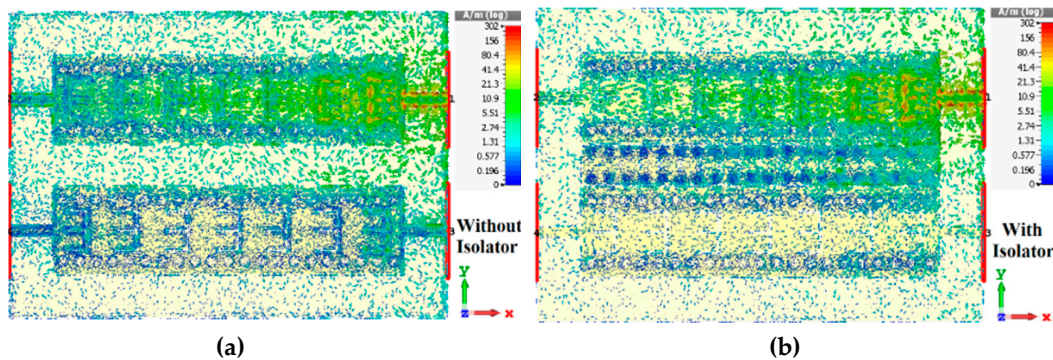
Figure 8. Surface current density distributions without and with the metamaterial shield at 60 GHz. (**a**) without the metamaterial shield; (**b**) with the metamaterial shield.

4. Circuit Model of The Proposed MTM-Lwa Array and its Dispersion Phenomenon

One way to explain the metamaterials (MTMs) is the transmission-line theory in terms of the circuit models. The concept of the composite right/left-handed metamaterial transmission lines (CRLH-MTM TLs) is investigated and realized based on this approach. This solution has been broadly recognized and adopted as a powerful analysis tool for the understanding and modelling of MTM devices. By considering the right-handed (RH) effects within a purely left-handed (LH) circuit, it demonstrates a general configuration of a practical MTM-TL. The circuit model of a generic symmetrical CRLH transmission-line unit-cell has exhibited in Figure 9 where the loss is neglected

for simplicity. The series capacitance (C_L) and the shunt inductance (L_L), which have been realized by the slots and via-holes, respectively, contribute to the left-handedness while the series inductance (L_R) and the shunt capacitance (C_R), which have been implemented by the unwanted currents flowing on the patches and the gap space between the patches and ground plane, respectively, actualize its right-handed (RH) dual counterpart. The one indicated in Figure 9a is called T-type model with the LH capacitance placed at the two ends. The mushroom unit cell belongs to this type [14]. The circuit exhibited in Figure 9b is called π-type model with the LH capacitance in the centre. One example is the CRLH-SIW unit cell [15–17]. Therefore, each unit cell of the proposed leaky wave array antennas is based on the π-type model, which has been identified in Figure 4b.

(a)   (b)
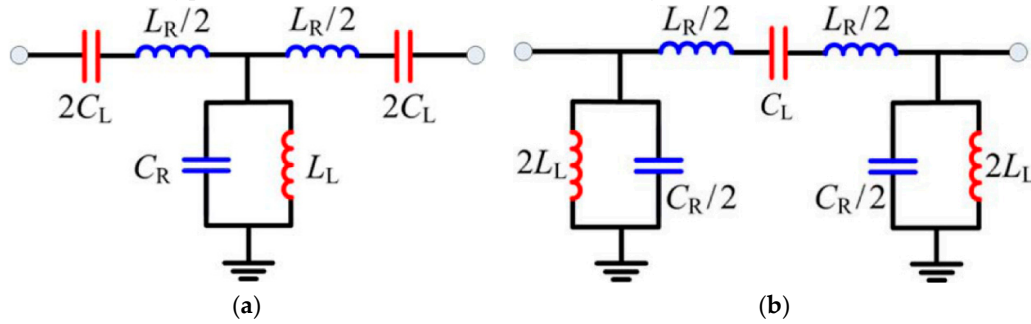
Figure 9. Equivalent circuit models for the symmetrical CRLH-metamaterial unit-cells. (**a**) T-type circuit model. (**b**) π-type circuit model.

By using the periodic boundary conditions corresponding to the Bloch–Floquet theorem, these two CRLH transmission line unit-cells basically become equal and their dispersion relevance is determined to be [9]:

$$\beta(\omega) = \frac{1}{p}\cos^{-1}(1 - \frac{1}{2}(\frac{\omega_L^2}{\omega^2} + \frac{\omega^2}{\omega_R^2} - \frac{\omega_L^2}{\omega_{se}^2} - \frac{\omega_L^2}{\omega_{sh}^2}))$$

(1)

where p = 5 mm is the length of the unit-cell and

$$\omega_L = \frac{1}{\sqrt{C_L L_L}}$$

(2)

$$\omega_R = \frac{1}{\sqrt{C_R L_R}}$$

(3)

$$\omega_{se} = \frac{1}{\sqrt{C_L L_R}}$$

(4)

$$\omega_{sh} = \frac{1}{\sqrt{C_R L_L}}$$

(5)

Seemingly, there are two frequency spots referred to as the infinite-wavelength points ($\beta = 0$) with a bandgap in between. In the balanced case ($\omega_{se} = \omega_{sh}$), the bandgap vanishes. Generally, just one particular zeroth-order resonance will be excited that depends on the boundary conditions and the circuit values. For the short-ended resonator, it is determined by ω_{se}, while for the open-ended case, it is represented by ω_{sh} [9]. Multiplex resonances containing the negative-, zeroth-, and positive- order resonances can be produced by cascading more than one unit-cell. Those resonance frequencies of different order modes for an M-stage CRLH-transmission line can be discovered on the dispersion diagram when the following condition is satisfied [9]:

$$\theta_M = \beta p_M = \beta M_p = n\pi$$

(6)

$$\beta p = \frac{n\pi}{M} \begin{cases} n = 0, \pm 1, \dots, \pm(M-1), for\ T\ type\ unice\ cell \\ n = 0, \pm 1, \dots, \pm M, for\ \pi\ type\ unice\ cell\ . \end{cases}$$

(7)

The proposed leaky wave antenna (LWA) array applying the CRLH-SIW unit-cell as shown in Figures 1 and 4 has an π-type circuit model with the two ends terminated by the LH inductances (L_L) realized by the metallic via-holes. The E-shaped transverse and the tapered transverse slots have presented within the circuit model as the LH capacitances (C_L). RH contribution comes from the distributed shunt capacitor (C_R) and the series inductor (L_R). Figure 10 shows the dispersion curves of the proposed leaky wave array antennas based on the CRLH-SIW unit-cell that has been extracted by the CST Microwave Studio package and the equivalent circuit model exhibited in Figure 9b. It has been observed that the results achieved from CST Microwave Studio package and the circuit elements are in an excellent coherence with each other, and also it illustrates the dispersion relation of the unit-cell very well. There is one zeroth-order resonance frequency occurring at 61 GHz that defines the upper and lower edges of the stop-band. This LW antenna array falls into the short-ended case because it is operated below the original waveguide cutoff-frequency and the metallic via-holes offer the short-ended condition. According to Equations (6) and (7), there is one resonance that can be excited comprising the zeroth-order resonance at f_{se} = 61 GHz. Figure 5 shows the reflection coefficient which has verified the proposed model. Notice that this resonance frequency can be simply controlled by engineering the dispersion diagram. Magnitudes of the equivalent circuit parameters, which were determined from full-wave EM simulation using CST Microwave Studio package, are L_L = 6.45 *nH*, C_L = 8.69 *pF*, L_R = 1.53 *nH*, and C_R = 4.12 *pF*. This data was then utilized to determine the equivalent circuit-model of the antenna, displayed in Figure 9b, which was verified applying ADS (RF-circuit solver).
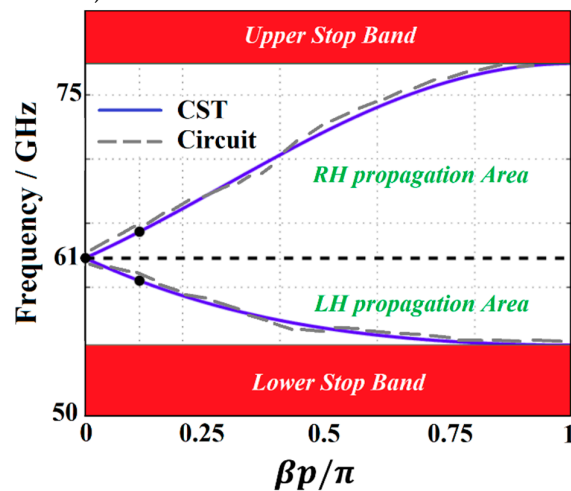
Figure 10. Dispersion diagrams for the proposed LWA array based on SIW-MTM extracted by CST Microwave Studio package and the corresponding equivalent circuit shown in Figure 9b.

The proposed LWA is exhibited as a traveling-wave antenna, where the current propagates along a guiding structure. Since that, the perturbations are introduced along the structure by implementing the E-shaped transverse and the traveling-wave leaves the structure and radiates into free-space. Therefore, in the ideal case, no energy reaches the end of the structure. In a practical scenario, any energy that reaches the end is absorbed by a matching load. Usually, LWA is designed, in which at the least 90% of the power at the structures leaks away before the traveling-waves reach the end of the antenna. Leaky-wave phenomenon is demonstrated with fast propagating waves only. The propagating wave number K_p is defined by [18,19]

$$K_p = \sqrt{K_0^2 - K_z^2} \tag{8}$$

In this case, $K_z = -j\alpha$ is for surface-wave or slow-wave, or $K_z = \beta$ is for leaky-wave or fast-wave, where K_z is the longitudinal wave-number and K_0 refers to the free-space propagating wave-number. The complexity of radiation K_z is given by

$$K_z = \beta - j\alpha \tag{9}$$

where α and β are the attenuation and phase constants respectively. Supposing that there is a standard free-space wave equation for the above wave, the waves outside the leaking-structure are given by:

$$\Psi(r) = \Psi_0 e^{-j(K_p p + \beta z)} e^{\alpha z} \tag{10}$$

If $\beta < K_p$ i.e. if the phase velocity is smaller than the free-space velocity of light, $V_p < C$, then it is a slow-wave and K_p is imaginary. The wave decays exponentially in amplitude along the length of the structure and it is a bounded wave. If, $\beta > K_p$ i.e. if the phase velocity is greater than the free space velocity of light, $V_p > C$, then it is a fast-wave and K_p is purely real; therefore, the real power at an angle is radiated with respect to the normal defined by [20]:

$$\sin(\theta) = sin^{-1}\left(\frac{\beta}{K_0}\right) = sin^{-1}\left(\frac{c\beta}{\omega}\right) \tag{11}$$

Since all of the abovementioned terms are functions of the angular frequency, the angle changes with frequency; hence, this shows frequency scanning behaviour. The main beam-width is

$$\Delta\theta_0 = \frac{0.91}{\left(\frac{l}{\lambda}\right)cos\theta_0} \tag{12}$$

If the above equation is applied for large antenna lengths, high directivity can be specified as

$$D = \frac{4\pi A_e}{\lambda_0} \tag{13}$$

However, the effect of enhancing directivity is negligible if there is no power left near the end of the structures. To specify this parameter, the attenuation/leakage constant is determined as [20]:

$$\alpha_z = \frac{e_r^{\frac{A^2(z)}{2}}}{\int_0^l A^2(z)dz - e_r \int_0^z A^2(z)dz} \tag{14}$$

Thus, if α is sufficiently small so that $(1 - e^{-2\alpha l} > 0)$, the improvement of directivity is perceptible as length l enhances.

5. Comparison between This Work and The Literature

Performance parameters of the proposed 1 × 2 MTM-LWA array antenna based on SIW is compared with the recent works employing various mutual coupling suppression techniques. The comparison in Table 3 is for array antennas composed of two radiation elements. Most of the arrays listed in Table 3 exhibit narrow band performance, and to increase isolation between the radiation elements they employ defected ground structures (DGS) to complement their suppression technique. The proposed array antenna presented here has the advantage of (i) symmetry; (ii) very wide bandwidth from 55 GHz to 65 GHz; (iii) simple design; (iv) improved radiation patterns; (v) enhanced radiation gain; (vi) low cross-polarization levels; and (vii) mutual coupling suppression on average of ~25dB over its operating band.

Table 3. Performance parameters of the proposed lw array antennas in comparison with the recent papers.

Ref.	Method	Max. isolation improvement	Bandwidth (FBW)	Rad. gain pattern deterioration	No. of elements	Application of DGS	Symmetry and Simplicity
[21]	SCSRR	10 dB	Narrow	Yes	2	Yes	No
[22]	SCSSRR	14.6 dB	Narrow	Yes	2	Yes	No

[23]	Compact EBG	17 dB	Narrow	Yes	2	Yes	No
[24]	Fractal MTM-EMBG	37 dB	Wide (~15%)	No	4	No	Yes
[25]	Meander Line	10 dB	Narrow	No	2	Yes	No
[26]	EBG	8.8 dB	Narrow	-		Yes	No
[27]	EBG	13 dB	Wide (~12%)	Yes	2	Yes	No
[28]	Substrate Integrated Waveguide (SIW) with Transverse Slots	15 dB	Wide (22.22%)	-	1	No	Yes
[29]	Substrate Integrated Waveguide (SIW) and Slots	20 dB	Wide (16.32%)	-	1	No	Yes
[30]	Periodic Space-Time Modulation	-	Wide (58.82%)	-	1	No	Yes
[31]	Space Time Modulation (External Linear Momentum)	-	-	-	1	No	Yes
[32]	MTM-DS	57 dB	Wide	No	2	No	Yes
[33]	Fractal load + DGS	16 dB	Narrow (2.5%)	No	2	Yes	No
[34]	Slotted Meander-Line	16 dB	Narrow	Yes	2	Yes	No
[35]	Slots	>26 dB	Wide	No	4	No	Yes
[36]	I-Shaped Resonator	30dB	Narrow	Yes	2	Yes	No
[37]	W/g MTM	18 dB	Narrow	No	2	Yes	No
[38]	MSWI	13.5 dB	Wide	No	2	No	Yes
[39]	Metamaterial Superstrate	25	Narrow	No	2	No	Yes
[40]	Slot Combined Complementary Split Ring Resonator	19	Narrow	Yes	2	No	No
[41]	Metamaterial	40	Wide (8.8%)	No	4	No	Yes
[42]	Fractal Load	37	Wide	No	2	No	Yes
This work	Metamaterials and Substrate Integrated Waveguide	42.5 dB	Wide (16.66%)	No	2	No	Yes

6. Conclusion

A feasibility study of a new metamaterial leaky-wave array antenna based on substrate-integrated waveguide (SIW) technology with transverse slots and metallic via-holes for operation over 55 GHz to 65 GHz was proposed and investigated. The array antenna provides beam-scanning capability of ±30° with the gain of 8.5, 10.1, and 9.5 dBi at backward (-30°), broadside (0°), and forward (+30°) directions, respectively. To increase the isolation between the array's elements, a metamaterial shield based on SIW was introduced between the antennas, which has reduced the mutual coupling by an average value of ~25 dB. In addition, the proposed MTM shield has increased the radiation gain and efficiency by an average value of ~1dBi and ~13%, respectively.

Author Contributions: Conceptualization, Mohammad Alibakhshikenari; Bal Singh Virdee; Francisco Falcone; Ernesto Limiti; methodology, Mohammad Alibakhshikenari; Chan H. See; Francisco Falcone; Ernesto Limiti; software, Mohammad Alibakhshikenari; Bal Singh Virdee; Chan H. See; validation, Mohammad Alibakhshikenari; Bal Singh Virdee; Chan H. See; Raed A. Abd-Alhameed; Francisco Falcone; Ernesto Limiti;

formal analysis, Mohammad Alibakhshikenari; Bal Singh Virdee; Francisco Falcone; Ernesto Limiti; investigation, Mohammad Alibakhshikenari; Bal Singh Virdee; Chan H. See; Raed A. Abd-Alhameed; Francisco Falcone; Ernesto Limiti; resources, Mohammad Alibakhshikenari; Chan H. See; Raed A. Abd-Alhameed; Ernesto Limiti; data curation, Mohammad Alibakhshikenari; Chan H. See; Raed A. Abd-Alhameed; Francisco Falcone; writing—original draft preparation, Mohammad Alibakhshikenari; writing—review and editing, Bal Singh Virdee; Chan H. See; Raed A. Abd-Alhameed; Francisco Falcone; Ernesto Limiti; visualization, Mohammad Alibakhshikenari; Bal Singh Virdee; Chan H. See; Francisco Falcone; Ernesto Limiti; supervision, Ernesto Limiti; project administration, Raed A. Abd-Alhameed; Francisco Falcone; Ernesto Limiti; funding acquisition, Raed A. Abd-Alhameed; Francisco Falcone; Ernesto Limiti.

Conflicts of Interest: The authors declare no conflict of interest. The funders had no role in the design of the study; in the collection, analyses, or interpretation of data; in the writing of the manuscript, or in the decision to publish the results.

References

1. Jackson, D.R.; Oliner, A.A. Leaky-wave antennas. In *Modern Antenna Handbook*; John Wiley & Sons: New York, NY, USA, 2008; pp. 325–367.
2. Sievenpiper, D.F. Forward and backward leaky wave radiation with large effective aperture from an electronically tunable textured surface. *IEEE Trans. Antennas Propag.* **2005**, *53*, 236–247.
3. Jackson, D.R.; Caloz, C.; Itoh, T. Leaky-wave antennas. *Proc. IEEE* **2012**, *100*, 2194–2206.
4. Lim, S.; Caloz, C.; Itoh, T. Metamaterial-based electronically controlled transmission-line structure as a novel leaky-wave antenna with tunable radiation angle and beamwidth. *IEEE Trans. Microw. Theory Tech.* **2004**, *52*, 2678–2690.
5. Caloz, C.; Itoh, T.; Rennings, A. CRLH metamaterial leaky-wave and resonant antennas. *IEEE Antennas Propag. Mag.* **2008**, *50*, 25–39.
6. Paulotto, S.; Baccarelli, P.; Frezza, F.; Jackson, D.R. A novel technique for open-stopband suppression in 1-D periodic printed leaky-wave antennas. *IEEE Trans. Antennas Propag.* **2009**, *57*, 1894–1906.
7. Chen, Z.N.; Qing, X. Slotted SIW Leaky-Wave Antenna with Improved Backward Scanning Bandwidth and Consistent Gain. In Proceedings of the 2017 11th European Conference on Antennas and Propagation (EUCAP), Paris, France, 19–24 March 2017; pp. 752–755.
8. Qian, Y.; Chang, B.C.C.; Itoh, T.; Chen, K.C.; Tzuang, C.K.C. High efficiency and broadband excitation of leaky mode in microstrip structures. In Proceedings of the 1999 IEEE MTT-S International Microwave Symposium Digest (Cat. No.99CH36282), Anaheim, CA, USA, 13–19 June 1999; pp. 1419–1422.
9. Caloz, C.; Itoh, T. *Electromagnetic Metamaterials: Transmission Line Theory and Microwave Applications*; Wiley-IEEE Press: New York, NY, USA, 2005, 376 Pages.
10. Yang, T.; Chi, P.L.; Xu, R.M. Novel composite right/left-handed leaky-wave antennas based on the folded substrate-integrated waveguide structures. *Prog. Electromagn. Res.* **2012**, *29*, 235–248.
11. Dong, Y.; Itoh, T. Composite right/left-handed substrate integrated waveguide and half mode substrate integrated waveguide leaky-wave structures. *IEEE Trans. Antennas Propag.* **2011**, *59*, 767–775.
12. Weitsch, Y.; Eibert, T.F. Analysis and design of a composite left/right-handed leaky wave antenna based on the H10 rectangular waveguide mode. *Adv. Radio Sci.* **2008**, *6*, 49–54.
13. Chen, Z.N.; Qing, X. Multilayered composite right/left-handed leaky-wave antenna with consistent gain. *IEEE Trans. Antennas Propag.* **2012**, *60*, 5056–5062.
14. Lai, A.; Leong, K.M.; Itoh, T. Infinite wavelength resonant antennas with monopolar radiation pattern based on periodic structures. *IEEE Trans. Antennas Propag.* **2007**, *55*, 868–876.
15. Dong, Y.; Itoh, T. Miniaturized substrate integrated waveguide slot antennas based on negative order resonance. *IEEE Trans. Antennas Propag.* **2010**, *58*, 3856–3864.
16. Dong, Y.; Itoh, T. Substrate integrated waveguide negative order resonances and their applications. *IEEE Trans. Antennas Propag.* **2010**, *4*, 1081–1091.
17. Dong, Y.; Itoh, T. Metamaterial-Based Antennas. *Proc. IEEE* **2012**, *100*, 2271–2285.
18. Johnson, R.C.; Jasik, H. *Antenna Engineering Handbook*, 4th ed.; McGraw-Hill Education: New York, NY, USA, 2007.

19. Mohsen, M.K.; Isa, M.S.M.; Isa, A.A.M.; Zin, M.S.I.M.; Saat, S.; Zakaria, Z.; Ibrahim, I.M.; Abu, M.; Ahmad, A.; Abdulhameed, M.K. The Fundamental of Leaky Wave Antenna. *J. Telecommun. Electron. Comput. Eng.* **2018**, *10*, 19–127.

20. Frank, B.G. *Frontiers in Antennas: Next Generation Design & Engineering*; McGraw Hill Professional: New York, NY, USA, Dec 22, 2010; 512 pages.

21. Bait-Suwailam, M.M.; Siddiqui, O.F.; Ramahi, O.M. Mutual coupling reduction between microstrip patch antennas using slotted-complementary split-ring resonators. *IEEE Antennas Wirel. Prop. Lett.* **2010**, *9*, 876–878.

22. Shafique, M.F.; Qamar, Z.; Riaz, L.; Saleem, R.; Khan, S.A. Coupling suppression in densely packed microstrip arrays using metamaterial structure. *Microw. Opt. Tech. Lett.* **2015**, *57*, 759–763.

23. Islam, M.T.; Alam, M.S. Compact EBG Structure for Alleviating Mutual Coupling between Patch Antenna Array Elements. *Prog. Electromagn. Res.* **2013**, *137*, 425–438.

24. Alibakhshikenari, M.; Virdee, B.S.; See, C.H.; Abd-Alhameed, R.; Ali, A.H.; Falcone, F.; Limiti, E. Study on Isolation Improvement Between Closely Packed Patch Antenna Arrays Based on Fractal Metamaterial Electromagnetic Bandgap Structures. *IET Microw. Ant. Propag.* **2018**, *12*, 2241–2247.

25. Ghosh, T.; Ghosal, S.; Mitra, D.; Bhadra Chaudhuri, S.R. Mutual Coupling Reduction Between Closely Placed Microstrip Patch Antenna Using Meander Line Resonator. *Prog. Electromag. Res. Lett.* **2016**, *59*, 115–122.

26. Yang, F.; Rahmat-Samii, Y. Microstrip Antennas Integrated with Elctromagnetic Band-Gap (EBG) Structures: A Low Mutual Coupling Design for Array Applications. *IEEE Trans. Antennas Propag.* **2003**, *51*, 2936–2946.

27. Mu'ath, J.; Denidni, T.A.; Sebak, A.R. Millimeter Wave Compact EBG Structure for Mutual Coupling Reduction Applications. *IEEE Trans. Antennas Propag.* **2015**, *63*, 823–828.

28. Liu, J.; Jackson, D.R.; Long, Y. Substrate integrated waveguide (SIW) leaky-wave antenna with transverse slots. *IEEE Trans. Antennas Propag.* **2012**, *60*, 20–29.

29. Ettorre, M.; Sauleau, R.; Le Coq, L. Multi-beam multi-layer leaky-wave SIW pillbox antenna for millimeter-wave applications. *IEEE Trans. Antennas Propag.* **2011**, *59*, 1093–1100.

30. Taravati, S.; Caloz, C. Mixer-duplexer-antenna leaky-wave system based on periodic space-time modulation. *IEEE Trans. Antennas Propag.* **2017**, *65*, 442–452.

31. Taravati, S.; Caloz, C. Space-time modulated nonreciprocal mixing, amplifying and scanning leaky-wave antenna system. In Proceedings of the 2015 IEEE International Symposium on Antennas and Propagation & USNC/URSI National Radio Science Meeting, Vancouver, BC, Canada, 19–24 July 2015; pp. 639–640.

32. Alibakhshikenari, M.; Virdee, B.S.; Shukla, P.; See, C.H.; Abd-Alhameed, R.; Khalily, M.; Falcone, F.; Limiti, E. Interaction Between Closely Packed Array Antenna Elements Using Metasurface for Applications Such as MIMO Systems and Synthetic Aperture Radars. *Radio Sci.* **2018**, *53*, 1368–1381.

33. Yang, X.; Liu, Y.; Xu, Y.X.; Gong, S.X. Isolation Enhancement in Patch Antenna Array with fractal UC-EBG Structure and Cross Slot. *IEEE Antennas Wirel. Propag. Lett.* **2017**, *16*, 2175–2178.

34. Alsath, M.G.N.; Kanagasabai, M.; Balasubramanian, B. Implementation of Slotted Meander Line Resonators for Isolation Enhancement in Microstrip Patch Antenna Arrays. *IEEE Antennas Wirel. Propag. Lett.* **2013**, *12*, 15–18.

35. Alibakhshikenari, M.; Virdee, B.; Shukla, P.; See, C.; Abd-Alhameed, R.; Khalily, M.; Falcone, F.; Limiti, E. Antenna Mutual Coupling Suppression Over Wideband Using Embedded Periphery Slot for Antenna Arrays. *Electronics* **2018**, *7*, 198, doi:10.3390/electronics7090198.

36. Ghosh, C.K.; Parui, S.K. Reduction of Mutual Coupling Between E-Shaped Microstrip Antennas by Using a Simple Microstrip I-Section. *Microw. Opt. Tech. Lett.* **2013**, *55*, 2544–2549.

37. Qamar, Z.; Park, H.C. Compact Waveguided Metamaterials for Suppression of Mutual Coupling in Microstrip Array. *Prog. Electromagn. Res.* **2014**, *149*, 183–192.

38. Alibakhshikenari, M.; See, C.H.; Virdee, B.S.; Abd-Alhameed, R.A. Meta-surface Wall Suppression of Mutual Coupling between Microstrip Patch Antenna Arrays for THz-band Applications. *Prog. Electromagn. Res. Lett.* **2018**, *75*, 105–111.

39. Qamar, Z.; Naeem, U.; Khan, S.A. Mutual coupling reduction for high performance densely packed patch antenna arrays on finite substrate. *IEEE Trans. Antennas Propag.* **2016**, *64*, 1653–1660.

40. Qamar, Z.; Riaz, L.; Chongcheawchamnan, M.; Khan, S.A.; Shafique, M.F. Slot combined complementary split ring resonators for mutual coupling suppression in microstrip phased arrays. *IET Microw. Antenna Propag.* **2014**, *8*, 1261–1267.

41. Alibakhshikenari, M.; Khalily, M.; Virdee, B.S.; See, C.H.; Abd-Alhameed, R.A.; Limiti, E. Mutual-Coupling Isolation Using Embedded Metamaterial EM Bandgap Decoupling Slab for Densely Packed Array Antennas. *IEEE Access* **2019**, *7*, 5182–51840.

42. Alibakhshikenari, M.; Khalily, M.; Virdee, B.S.; See, C.H.; Abd-Alhameed, R.A.; Limiti, E. Mutual Coupling Suppression Between Two Closely Placed Microstrip Patches Using EM-Bandgap Metamaterial Fractal Loading. *IEEE Access* **2019**, *7*, 23606–23614.